Am J Cancer Res 2024;14(4):1501-1522
www.ajcr.us /ISSN:2156-6976/ajcr0155599

Original Article

Transcription factor STAT4 counteracts radiotherapy resistance in breast carcinoma cells by activating the MALAT1/miR-21-5p/THRB regulatory network

Leiming Guo*, Gaofeng Ding*, Yuntao Ba, Bo Tan, Lingling Tian, Kunlun Wang

*Department of Radiation, The Affiliated Cancer Hospital of Zhengzhou University & Henan Cancer Hospital, Zhengzhou 450008, Henan, China. *Equal contributors and co-first authors.*

Received January 23, 2024; Accepted March 31, 2024; Epub April 15, 2024; Published April 30, 2024

Abstract: Considering the limited research and the prevailing evidence of STAT4's tumor-suppressing role in breast carcinoma (BC) or in breast radiotherapy (RT) sensitivity requires more in-depth exploration. Our study delves into how STAT4, a transcription factor, affects BC cell resistance to radiotherapy by regulating the MALAT1/miR-21-5p/THRB axis. Bioinformatics analysis was performed to predict the regulatory mechanisms associated with STAT4 in BC. Subsequently, we identified the expression profiles of STAT4, MALAT1, miR-21-5p, and THRB in various tissues and cell lines, exploring their interactions and impact on RT resistance in BC cells. Moreover, animal models were established with X-ray irradiation for further validation. We discovered that STAT4, which is found to be minimally expressed in breast carcinoma (BC) tissues and cell lines, has been associated with a poorer prognosis. *In vitro* cellular assays indicated that STAT4 could mitigate radiotherapy resistance in BC cells by transcriptional activation of MALAT1. Additionally, MALAT1 up-regulated THRB expression by adsorbing miR-21-5p. As demonstrated *in vitro* and *in vivo*, overexpressing STAT4 inhibited miR-21-5p and enhanced THRB levels through transcriptional activation of MALAT1, which ultimately contributes to the reversal of radiotherapy resistance in BC cells and the suppression of tumor formation in nude mice. Collectively, STAT4 could inhibit miR-21-5p and up-regulate THRB expression through transcriptional activation of MALAT1, thereby mitigating BC cell resistance to radiotherapy and ultimately preventing BC development and progression.

Keywords: Breast carcinoma, radiotherapy resistance, transcription factor, STAT4, long non-coding RNA, MALAT1, microRNA-21-5p, THRB

Introduction

Breast carcinoma (BC), one of the most pervasive malignancies, afflicts over 2 million new cases worldwide yearly with a higher prevalence in developed countries. In the United States, BC is the most frequently diagnosed tumor in women, ranking 2rd leading cause of cancer-related mortality among women [1, 2]. Traditional BC diagnosis includes imaging, pathology and molecular markers such as ER and HER2. Research is expanding into novel diagnostic tools, such as new molecular markers, including miRNAs in situ and in plasma, and tumor stem cell expression profiles [3, 4]. Traditional treatments include surgery and radiotherapy treatment, but the medical field has advanced to embrace new therapies including newer versions of old drugs (e.g. mTOR inhibitors) and fractionated chemotherapy (i.e. continuous, regular and low-dose chemotherapy for cancer patients) [5].

STAT4, known as signal transduction transcription activator 4, is a transcriptional activator that enters the nucleus of cells to promote gene transcription. In humans, STAT4 is a key immune regulator involved in the transcription of various immune cytokines, such as IL-12 and IFN-I [6, 7]. Reports have linked abnormal STAT4 expression to the progression of diseases like systemic lupus erythematosus and hepatocellular carcinoma [8]. However, the correlation between STAT4 and BC progression is underexplored,

https://doi.org/10.62347/VSJU7227

with limited reports suggesting that STAT4 is lowly expressed in BC tissues and high STAT4 level may correlate with improved outcome [9, 10]. Meanwhile, STAT family constitute cellular differentiation, development, proliferation, apoptosis, inflammation, and other biological functions after being activated by specific cytokines [11]. Among the members, the inhibition of STAT1 was found to sensitize renal cell carcinoma cell lines to radiotherapy and chemotherapy, while STAT3 has been shown to be involved in resistance to radiotherapy [12, 13]. Given the structural and sequence similarities of STAT4 and STAT3, STAT4 has the potential for a similar effect on radiotherapy resistance in BC, but has not yet been established in the research.

MALAT1, dysregulated in a variety of tumors [14], is a long-stranded non-coding ribose nucleic acid (RNA) that primarily exerts its function through regulating the subcellular localization of transcription factors, acting both as a cis and trans element in transcription and post-transcriptional modification, and serving as a miRNAs sponge [15, 16]. It plays a significant role in BC, as Kim et al. report that MALAT1 knockdown promotes BC metastasis. This indicates that MALAT1 is a lncRNA that inhibits BC metastasis [17].

miR-21-5p, a microRNA (miRNA), represses the expression of its downstream target genes by preventing their binding to the 3' untranslated region (UTR) sequence [18]. According to reports, miR-21-5p presents abnormal expression in BC [19], and its up-regulation can act as a molecular marker for BC metastasis [20]. Given the high miR-21 expression in plasma exosomes, it is possible to diagnose BC by measuring miR-21 levels in exosomes [21]. miR-211 is not only involved in BC development but is also closely related to its chemoresistance [22].

THRB, thyroid hormone receptor beta, is the thyroid hormone receptor and plays a vital part in the physiological function of thyroid hormones. As thyroid hormones are closely related to neurodevelopment, this regulation of this gene also affects brain development and function [23]. In addition, THRB promotes stem cell differentiation into hepatocytes [24], and its deletion has been linked to various cancers [25]. THRB heterozygous deletion has been strongly associated with the development of invasive BC [26], and other research has also indicated that mutations in THRB are more likely to contribute to the development of BC [27].

Building on the evidence gathered, we hypothesized that STAT4 may affect BC radiotherapy resistance and set out to explore its mechanism of action through a series of experiments. This work aims to reveal the role of STAT4/MALAT1/miR-21-5p/THRB axis in BC radiotherapy resistance and the specific molecular mechanisms. The insights from this study have the potential to inspire fresh avenues in both basic and clinical research on BC, identify novel targets for clinical treatment interventions, and ultimately enhance the therapeutic outcomes and prognosis for patients with BC.

Materials and methods

Sampling

We included sixty-six patients aged between 40 and 69 years (48.67 ± 6.38), all of whom underwent surgical treatment in our hospital from December 2020 to January 2021 and had postoperative pathologically confirmed BC. These patients did not receive any preoperative treatment including radiotherapy and chemotherapy. During the procedure, we obtained cancer tissue specimens from the non-necrotic bleeding area in the tumor center and paracancer tissue specimens from the normal area of the distal 2 cm, and refrigerated them at -80°C for later gene and protein expression analysis [28]. In addition, patient basic data was collected from medical records. All cases underwent follow-ups for detailed information on post-treatment and clinical outcomes and improving their clinical profiles. The correlation of overall survival (OS) with gene expression was visualized by Kaplan-Meier (KM) curves. Analyses of the relationships between gene expression profiles employed Pearson correlation coefficients. All cases in this study were discussed and ratified by our medical ethics committee, and informed consent for the study was obtained. The guidelines specified in the *Declaration of Helsinki* were followed during the research.

Bioinformatics analysis

Gene differential analysis was performed on BC samples from the TCGA database by the bioinformatics tool GEPIA (http://gepia2.can-

cer-pku.cn/#index), setting *p*-value < 0.01 and |logFC| > 1 as the differentially expressed gene (DEG) screening threshold. DEGs (lncRNAs) were selected for further analysis, and the co-expression correlation of Sp1 with DEGs in BC was identified using Chipbase v2.0 (URL: http://rna.sysu.edu.cn/chipbase/). To predict the downstream regulators of LncRNAs, we used StarBase (URL: https://starbase.sysu.edu.cn/) and LncBase (URL: https://diana.e-ce.uth.gr/lncbasev3/home) to predict their downstream miRNAs. We also employed the GeneCards database (URL: https://www.genecards.org/) to identify BC-related genes and screen out their miRNAs. We used the Sangerbox website (URL: http://vip.sangerbox.com/home.html) to take the predicted miRNAs and BC intersection of predicted and relevant miRNAs. Further, miRDB (URL: https://mirdb.org/mirdb/index.html), mirT-CDS (URL: https://dianalab.e-ce.uth.gr/html/dianauniverse/index.php?r=MicroT_CDS/index), mirDIP (URL: http://ophid.utoronto.ca/mirDIP/) and StarBase were made use of to predict the miRNAs' target genes, using the Sangerbox website to take the intersections and to predict the binding sites of the miRNAs to the mRNAs.

Real-time fluorescent quantitative PCR (RT-qPCR)

Total tissue and cellular RNA was isolated using the TRIzol (Invitrogen, Calsbad, CA, USA) method, and its concentration and purity were assessed with a nanodrop2000 micro UV spectrophotometer (1011U, Nanodrop, USA). The conversion of mRNA to cDNA was facilitated by a reverse transcription kit (RR047A) purchased from Takara, Japan. miRNAs were measured using a PolyA plus tailing assay kit (B532451, Biotech, China) for cDNA synthesis. Primer design and synthesis for STAT4, MALAT1, miR-21-5p and THRB were also courtesy of Takara. RT-qPCR was conducted using the TaqMan Multiplex RT-qPCR Solution (4461882, Thermo, USA) and an ABI7500 qPCR instrument (7500, ABI, USA), as following reaction conditions: 95°C pre-denaturation (10 min), 95°C denaturation (10 s), 60°C annealing (20 s), and 72°C extension (34 s) for 40 cycles, and analysis of PCR product melting curves by 65°C-95°C. The relative expression levels of the target genes, normalized to GAPDH and U6, were quantified utilizing the $2^{-\Delta\Delta CT}$ [29].

Western blot (WB)

Tissues or cells from each group were lysed on ice for 10 minutes with a phenylmethanesulfonyl fluoride (PMSF)-enhanced radioimmunoprecipitation assay (RIPA) lysate (P0013B, Beyotime, China), followed by high-speed centrifugation for supernatant collection (14,000 rpm, 4°C). Protein concentrations were then determined using a BCA protein assay (ST2222, Beyotime, China). For immunoblotting, proteins were incubated with primary antibody overnight at 4°C and rinsed with PBST at an ambient temperature, following by room temperature incubation with secondary antibody (1 h). After culturing with ECL reaction solution (Thermo Fisher, USA), the immunoreactive proteins were visualized at room temperature. The protein blot images relative to GAPDH were analyzed using ImageJ2x [30]. The following antibodies were used in WB experiments: STAT4 (2653S, 1:1,000, Cell Signaling Technology, USA), GAPDH (ab9485, 1:1,000, Abcam, USA), horseradish peroxidase (HRP)-labelled rabbit IgG (sc-2357, 1:1,000, Santa Cruz, USA).

Cell screening, cultivation, and lentivirus transfection

Human BC SKBR3 (Item No. HTB-30), MDA-MB-231 (Item No. CRM-HTB-26), MCF-7 (Item No. CRL-3435), and MDA-MB-468 (Item No. HTB-132) cells, as well as normal MCF-10A mammary epithelial cells (Item No. CRL-10317) were purchased from ATCC (USA). The MCF-10A cell line, a control, was placed in Dulbecco's Modified Eagle's Medium (DMEM) and Ham's F12 medium (F12) (Gibco, USA) with 5% horse serum (Gibco, USA), 20 ng/mL epidermal growth factor (PeproTech, USA), 100 ng/mL cholera toxin (Sigma-Aldrich, USA), 10 μg/mL insulin (Sigma-Aldrich, USA), and 500 ng/mL hydrocortisone (Sigma-Aldrich, USA) for incubation, with 5% CO_2 in air and the temperature controlled at 37°C. A radiotherapy-resistant cell line of human BC cells was established using an X-ray gradient irradiation method: BC cells were immersed in 10% fetal bovine serum-supplemented RPMI-1640 based on 5% CO_2 (v/v) in a humidified incubator. After the BC cells had reached 50-60% density, the BC cells were irradiated with 2 Gy X-rays (dose-rate: 2.5 Gy/min) by using a Varian-6/100 linear accelerator purchased from Varian Medical Systems,

Inc., from Palo Alto, CA, USA. The culture solution was then changed to 10% fetal bovine serum-supplemented RPMI-1640, which was renewed every two days. The culture was performed using a 15% fetal bovine serum RPMI-1640 medium when multiple dying cells were observed. When cell growth after irradiation reaches 70~80% density. Irradiation was not discontinued unless a total dose of 60 Gy was reached. The cells finally collected were named MCF-7R, and the follow-up experiment was carried out after continuous culture for ≥ 2 weeks.

Cells were digested with trypsin at log phase, and inoculated with 1×10^5 cells per well in the wells of a 6-well plate for 24 h. The transfection was performed following the lipofectamin 2000 instructions (11668-019, Invitrogen, New York, California, USA) when reaching 50% confluence. The cells in logarithmic growth were seeded into a 6-well plate, and when the cell density reached 30%-50%, the cells were transfected according to the instructions of Lipofectamine 2000 (Invitrogen). 250 μL of serum-free medium Opti-MEM was used to diluted 100 pmol of each plasmid (final concentration was 50 nM) and 250 μL of Opti-MEM (serum-free) diluted with 5 μL of lipofectamine 2000, mixed thoroughly and added to 6-well plates after 20 min of standing. After transfection, cells were incubated under specific conditions (37°C, 5% CO_2, and saturated humidity). Cells were transfected in the following groups: oe-NC (negative control), oe-STAT4, MCF-7, MCF-7R+oe-NC, oe-MCF-7R+oe-STAT4, sh-MALAT1#1, sh-MALAT1#2, sh-MALAT1#3, oe-NC+sh-NC, oe-STAT4+sh-NC, oe-STAT4+sh NC, oe-STAT4+sh-MALAT1, MCF-7R+oe-NC+sh-NC, MCF-7R+oe-STAT4+sh-NC, MCF-7R+oe-STAT4+sh-MALAT, oe-MALAT1, sh-NC, sh-MALAT1, mimic NC, miR-21-5p mimic, inhibitor NC, miR-21-5p inhibitor, oe-NC+mimic NC, oe-NC+miR-21-5p mimic, oe-MALAT1+mimic NC, oe-MALAT1+miR-21-5p mimic, oe-STAT4+sh-THRB, and MCF-7R+oe-STAT4+sh-THRB groups. All overexpression or silencing plasmids, inhibitors and their NCs were ordered from Sino Biological (China). Cells were changed following transfection for 6 h and collected after culture 48 h for subsequent experiments [31, 32].

MTT assay

After a 5-minute centrifugation of the plates, the old culture medium was discarded, and cells were treated with MTT solution (1 mg/ml), freshly prepared and shielded from light, and incubated for 3 hours. Subsequently, plates were centrifuged for 6 minutes, MTT solution was removed, and DMSO (100 μl/well) was added, followed by 30 s of shaking on a shaker. An enzyme marker was then used to measure the 450-nm absorbance. Cell viability calculation formula: Cell viability = 100% × (the treated group's mean OD/the control group's mean OD) [33]. Experiments were run in triplicate in each group.

Plate clone formation experiments

Groups of BC cells during logarithmic growth were trypsin (0.25%)-digested and gently pipetted to make single cells, counted as live cells, and adjusted to 1×10^6 cells/mL. In each group, cells were inoculated into the wells of a 24-well plate (500 cells/well) where 1 mL of pre-warmed (37°C) culture medium was placed into each well, and gently rotated for even distribution of the cells. This was followed by a 2-3 week incubation period at 37°C with 5% CO_2, during which the medium was refreshed every two or three days. Cell growth was regularly observed, and the culture was terminated when clones were visible. Discard the supernatant and wash carefully with PBS 2 times. Cells were fixed with 5 mL of 4% paraformaldehyde for 15 min, then the fixative was removed, and the cells were wash twice with PBS. GIMSA stain was applied for 10-30 minutes, after which the stain was gently rinsed off with running water, and the dishes were allowed to air dry. Clone counting was then carried out by photographing the dishes with an inverted microscope (DMi8-M) purchased from Leica, Germany. Clones with more than 50 cells were counted as valid clones. Clone formation efficiency (%) = the number of clones formed/number of cells inoculated × 100%, Survival fraction (%) = clone formation rate of irradiated cells/clone formation rate of control cells × 100% [34]. Each set of experiments was run in triplicate.

Flow cytometry

For apoptosis detection by Annexin V-FITC/PI double staining and flow cytometry, the protocol is as follows: After removing culture medium, cells were rinsed once with pre-chilled PBS (4°C), trypsin-digested, and collected into a 15

mL centrifuge tube for centrifugation at 800 g/min. The supernatant was discarded, and the cells were rinsed twice with PBS. This was followed by resuspending the cells in 500 μL binding buffer as the Annexin V-FITC Apoptosis Detection Kit I (556547) instructions. A further resuspension was done in 500 μL of binding buffer, to which FITC and PI (5 μL each) were added. After thorough mixing and a 15-minute incubation, apoptosis detection by flow cytometry (BD FACSCalibur) [35]. Each set of experiments was run in triplicate.

RNA pull-down assay

MALAT1-pull-down: Ribo biological (China) was responsible for the design and synthesis of MALAT1-WT and -Mut, biotin-labelled probes. Groups of BC cells were subjected to two rinses with pre-chilled PBS, lysis in a lysis buffer, and 2 h of room temperature cultivation with 3 μg of biotin-labelled MALAT1-WT and -Mut probes; M-280 streptavidin magnetic beads pre-coated with RNase-free and yeast tRNA (S3762, Sigma, St. Louis, MO, USA) were then added together for 4 h, so as to pull down the biotin-coupled RNA complex. Following five washes of the beads with a lysis buffer, the pull-down complex-bound miRs were isolated with a Trizol reagent and analyzed for miR-21-5p amounts using RT-qPCR assay. miR-21-5p-pull-down: Ribo biological (China) was responsible for the design and synthesis of miR-21-5p-WT and -Mut, biotin-labelled probes. The pull-down experiment was conducted the same as aforementioned, using Trizol reagent to separate the pull-down complex-bound RNAs and RT-qPCR assay to analyze the MALAT1 amount [36]. All experiments were run in triplicate.

ChIP assay

The cells collected from each group were incubated for 10 min at 37°C with 1% formaldehyde solution after discarding the original culture medium. Following dilution with a containing protease-inhibitor CHIP dilution buffer, the supernatant was cultivated with a blocking solution for half an hour with the temperature controlled at 4°C. Subsequently, a fraction of the supernatant was centrifuged for 1 min at 4°C and used as Input, while a portion of the rest was added to the STAT4 antibody (Rabbit, #2653, Cell Signaling Technology, USA). A portion was added to a NC IgG (ab172730, Rabbit, Abcam, China) and incubated overnight (4°C). Protein G Dynabeads (10003D, Thermo Fisher, USA) were added and incubated (1 h at 4°C) to obtain the antibody/transcription factor complex. The supernatant was discarded by 1 min of centrifugation at 4°C, and the precipitate was washed well and eluted with elution buffer. In the eluted supernatant and Input DNA, 20 μL of NaCl (5 mol/L) was placed into the supernatant and Input DNA, respectively, followed by 4 h of immersion in a 65°C water bath for uncrosslinking. The recovered DNA was purified after protein removal by proteinase K digestion. The recovered DNA was used as a template to detect MALAT1 content using RT-qPCR [27, 37]. Each set of experiments was run in triplicate.

Dual-luciferase reporter (DLR) gene assay

Reporter plasmids MALAT1-WT and MALAT1-MUT were obtained by cloning the predicted binding site of MALAT1 with miR-21-5p and a mutated MALAT1 fragment into the Pmir-GLO Dual-Luciferase miRNA Target Expression Vector (Promega, USA). Similarly, reporter plasmids THRB-WT and THRB-MUT were prepared by inserting the predicted mRNA 3'-UTR binding site fragment of miR-21-5p with THRB and a mutated miR-21-5p fragment into the luciferase reporter vector. The mimic NC and miR-21-5p mimic were inserted into the MALAT1 and THRB luciferase reporter vectors, respectively. Subsequently, co-transfection of THRB luciferase reporter plasmids into 293T was carried out to test the ability of miR-21-5p to bind to MALAT1 and THRB. Sea pansy luciferase acted as an internal reference. Cell collection and lysis were performed 48 h post transfection with a DLR kit (E1910; Promega, USA). Sea pansy luciferase acted as an internal reference gene to compare target reporter gene activation based on the ratio obtained by dividing RLU (firefly luciferase assay value) by Renilla (sea pansy luciferase assay value) [38].

All reporter plasmids including pGL3-luc, pGL3-MALAT1-MUT-luc, and pGL3-MALAT1-WT-luc, were prepared by inserting the predicted MALAT1 promoter binding site fragment and mutant site fragment of STAT4 into the pGL3 Luciferase Reporter Vector (E1751, Promega, USA). Co-transfection of oe-NC and oe-STAT4 plasmids with MALAT1 promoter luciferase reporter plasmids into 293T (CRL-3216, ATCC,

USA) were carried out, respectively. The MALAT1 promoter activity was assessed as above. Each set of experiments was run in triplicate.

RIP assay

The basic steps of the Magna RIP RNA-Binding Protein Immunoprecipitation Kit (#17-700, Millipore, USA) are as follows: Cells are rinsed twice with pre-cooled PBS, collected with a cell scraper, and lysed in a buffer that includes ribonuclease and protease inhibitor (100 μL). After 30 min of lysis on ice and subsequent 30 min of centrifugation (4°C, 12000 g), the supernatant is collected. A small sample of this supernatant serves as the Input positive control, while the remaining supernatant was added protein A/G-beads (30 μl) and the corresponding antibody Anti-AGO_2 (Rabbit, ab186733, Abcam, USA; 1 μg) for cultivation overnight (4°C) with rotation. Following immunoprecipitation, the supernatant was discarded by centrifugation for 5 min under specific conditions (3000 g, 4°C). The protein A/G-beads were treated with thrice rinses with a lysis buffer (1 mL) and 1 min of centrifugation (1000 g, 4°C). Following the addition of a 2× SDS spiking buffer (15 μL) and metal bath heat treatment (10 min), the relevant RNAs were obtained, and MALAT1 and miR-21-5p were quantified by RT-qPCR [39, 40]. All experiments were run in triplicate.

Nude mice subcutaneous xenograft experiment

We purchased 48 SPF-grade male Balb/c nude mice of 5 weeks old and weighting 18-22 g from Viton Lever Laboratory Animal Technology Ltd. (Beijing, China) and housed them in a specific-pathogen-free animal facility individually, strictly following the guidelines in the Guide for the Care and Use of Laboratory Animals published by the National Institutes of Health. All animal experiments received approval from our animal ethics committee. MCF-7 BC cells, as well as MCF-7R+oe-NC+sh-NC, MCF-7R+oe-STAT4+sh-NC, and MCF-7R+oe-STAT4+sh-THRB group. MCF-7R BC cells were used for subcutaneous tumour formation experiments in the purchased animals. Using serum-free RPMI 1640 (Gibco, USA), BC cells were resuspended into a 1×10^6 cells/200 μL cell suspension and set aside. The animals were randomized into 4 groups of 12 each. After ether anaesthetization and routine sterilization, each animal was inoculated with 200 μL (1×10^6 cells) BC cells from the back of the right hind leg under the loose skin, and reared in the same environment. Once the average subcutaneous tumour size in each group reached 200 mm^3, the animals were subjected to a total of 4 Gy X-ray irradiation for five days. The mice were euthanized when the mean tumor size when the mean tumour diameter reached 1.5 cm. Tumor tissues were then excised, imaged, weighed, and their dimensions recorded [41, 42].

Immunohistochemical staining

Solid tumor tissues were embedded in paraffin and sectioned at 5 μm thickness. The tissue was routinely dewaxed in xylene (5 min/time for 3 times) and hydrated (100% alcohol hydration for 3 times, followed by 90%, 80%, and 70% alcohol, as well as PBS, once each for 5 min). After antigen retrieval utilizing a citrate buffer, 1% BSA solution was added for 1 h of room temperature sealing. Then came overnight culture with antibodies (anti-STAT4, ab284408, 1:500, Abcam, USA; rabbit anti-THRB, SAB4500820, 1:500; rabbit anti-ki67, SAB5700770, 1:100; Sigma, USA) at 4°C. The sections were then rinsed with PBS and cultivated with HRP-labelled IgG (sc 2357, Santa Cruz, USA) at an ambient temperature, 1 h. Colour development with DAB (AR1000, BOSTER, China) was terminated with tap water. Hematoxylin (G1004, Servicebio, China) stained nuclei were dehydrated in an alcohol gradient, blocked and examined microscopically [43].

Terminal deoxynucleotidyl transferase dUTP nick end labelling (TUNEL) detection of apoptosis

TUNEL was conducted as instructed by the manufacturer's recommendations (QIA39, Millipore, Sigma, USA). TUNEL-positive cells were observed and photographed using a fluorescent microscope (BX63, Olympus, Japan), in a randomized, double-blind manner. The TUNEL-positive cell count was calculated as a percentage of the total cell count [44].

Statistical methods

Data analyses were conducted using SPSS 21.0 from IBM, USA. Measures, described as

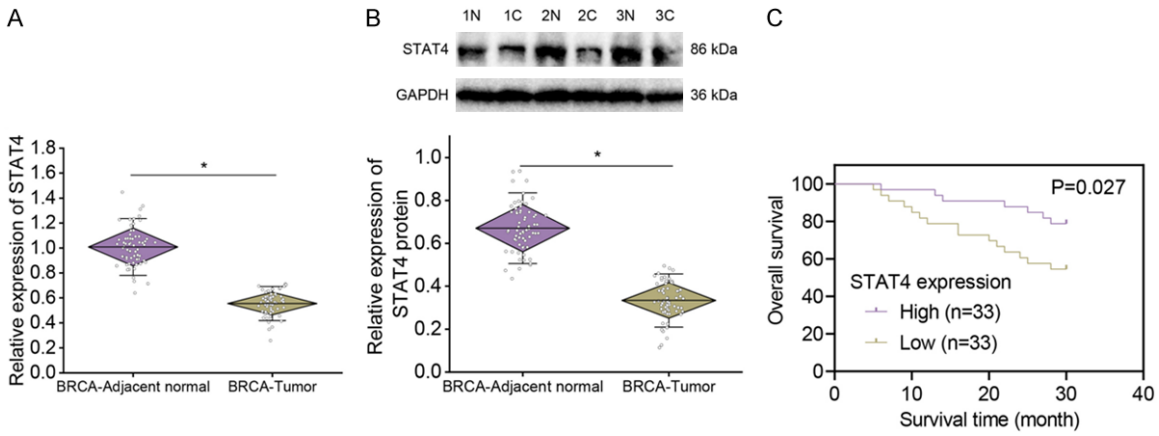

Figure 1. STAT4 expression in BC tissues. A, B: STAT4 mRNA and protein levels in cancerous and normal paracancerous tissues of BC patients by RT-qPCR and Western blot, n = 66, N indicates normal paracancerous tissue, C indicates BC tissue, * indicates comparison with normal paracancerous tissue, *$P < 0.05$; C: Kaplan-Meier curves display the correlation of STAT4 with patients' overall survival.

mean ± standard deviation, were comparatively analyzed between and among groups using unpaired t-tests and one-way ANOVA plus Tukey's post hoc tests, respectively. Multiple time-point comparisons employed repeated measures ANOVA as well as Bonferroni for post hoc tests. The KM method was used to calculate patient survival, and a one-way ANOVA was performed using the Log-rank test. Pearson correlation analysis was performed to observe the correlation of indicators. The significance level was $P < 0.05$.

Results

STAT4 is underexpressed in BC tissue and negatively correlates with adverse outcomes in BC patients

STAT4 has been found to be significantly underexpressed in various cancers, including ovarian cancer and liver cancer, and its expression is significantly associated with overall survival (OS) in cancer patients [45-47]. However, it has been relatively understudied in BC, with its mechanisms not fully elucidated. We quantified STAT4 protein and mRNA levels in both adjacent normal and BC tissues from 66 BC patients using Western Blot (WB) and RT-qPCR, observing substantially lower expression in BC tissues compared to adjacent normal tissues (**Figure 1A**, **1B**). Kaplan-Meier analysis of STAT4 expression's correlation with patient OS demonstrated notably longer OS in patients with higher STAT4 expression (**Figure 1C**).

STAT4 expression was downregulated in radiation therapy resistant BC cells

Using RT-qPCR and WB, we examined STAT4 levels in normal human MCF-10A mammary epithelial cells and four human BC cell lines (SKBR3, MDA-MB-231, MCF-7 and MDA-MB-468) to evaluate the role of STAT4 in BC cell resistance to radiotherapy. The results showed a marked downregulation of STAT4 mRNA and protein in SKBR3, MDA-MB-231, MCF-7 and MDA-MB-468 compared to MCF-10A, with MCF-7 cell line showing the lowest levels, prompting its selection for further study (**Figure 2A**, **2B**). Subsequently, we started to generate radiation therapy resistant cells. STAT4 mRNA and protein levels increased gradually with increasing X-ray doses from 0 Gy to 4 Gy but did not significantly change beyond this dose (**Figure 2C**, **2D**). Therefore, 4 Gy was selected as the irradiation dose.

RT-qPCR and WB further revealed gradually decreasing STAT4 mRNA and protein levels in MCF-7 with increasing irradiation time under X-ray irradiation at a dose level of 4 Gy (**Figure 2E**, **2F**). The radioresistant counterpart, MCF-7R, displayed notably lower STAT4 levels (**Figure 2G**, **2H**). Moreover, overexpression of STAT4 in MCF-7R cells was conducted to elucidate its impact on the cell tolerance to radiotherapy. As indicated by RT-qPCR and WB assays, oe-STAT4 group had notably higher STAT4 mRNA and protein levels than oe-NC group (**Figure 2I**, **2J**).

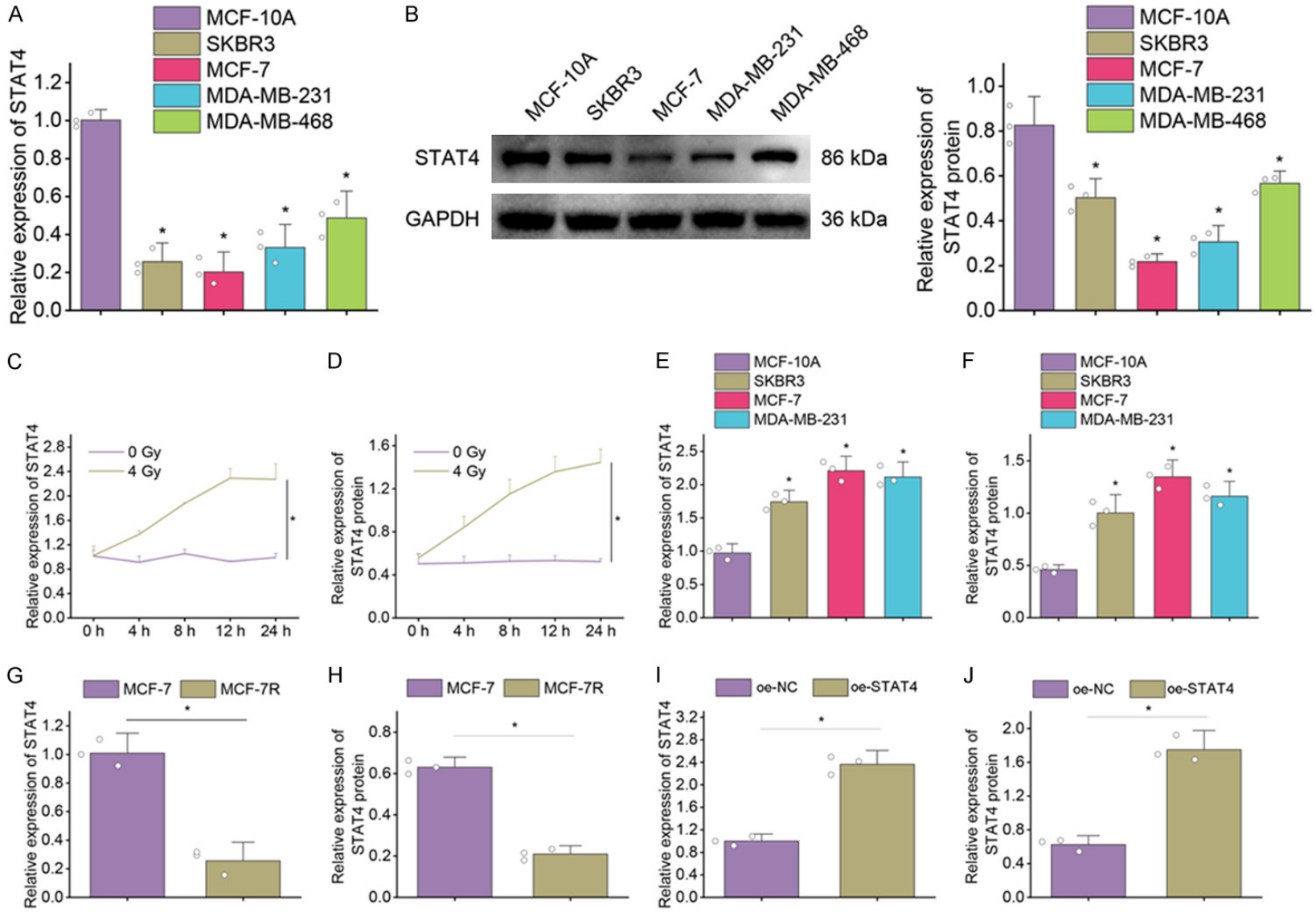

Figure 2. STAT4 expression was downregulated in radiation therapy resistant BC cells. A, B: STAT4 mRNA and protein levels in normal human MCF-10A mammary epithelial cells and four human BC cell lines (SKBR3, MDA-MB-231, MCF-7 and MDA-MB-468) by RT-qPCR and Western blot (WB); *$P < 0.05$ versus HBL-100 cells; C, D: RT-qPCR and WB for STAT4 mRNA and protein levels in MCF-7 at different time points after single-dose X-ray irradiation, *$P < 0.05$ versus 0 Gy group; E, F: STAT4 mRNA and protein levels in MCF-7 after X-ray irradiation of different doses by RT-qPCR and WB; G, H: RT-qPCR and WB for STAT4 mRNA and protein levels in MCF-7 and its corresponding radioresistant cell line MCF-7R, *$P < 0.05$ versus MCF-7 group; I, J: STAT4 mRNA and protein levels in MCF-7R in each group by RT-qPCR and WB, *$P < 0.05$ versus oe-NC group.

Overexpression of STAT4 inhibits radiotherapy resistance in BC cells

The survival of MCF-7, and MCF-7R in oe-NC and oe-STAT4 groups was measured by MTT assay at different time points (0 d, 1 d, 2 d, 3 d, 4 d) after 4 Gy X-ray irradiation. The cell proliferation ability was measured by plate cloning assay 24 h after X-rays. The results indicated that the cell survival rate (**Figure 3A**), proliferation ability (**Figure 3B**) were higher in MCF-7R+oe-NC group, while the apoptosis level were lower (**Figure 3C**). The survival rate (**Figure 3A**), proliferation ability (**Figure 3B**) of MCF-7R+oe-STAT4 cells were statistically lower versus MCF-7R+oe-NC cells and the apoptosis level were higher (**Figure 3C**). The plate cloning assay indicated that the proliferation capacity of MCF-7R cells in the oe-STAT4 group decreased more rapidly with higher doses of X-ray irradiation (**Figure 3D**). These results suggested that MCF-7R developed resistance to radiation, as its proliferation rate was significantly higher than that of MCF-7 cells. While overexpression of STAT4 could reduce the proliferation of MCF-7R cells, suggesting overexpression of STAT4 inhibits its radiotherapy resistance in BC cells.

STAT4 reverses BC cell resistance to radiotherapy activating MALAT1 expression

MALAT1, a long non-coding RNA, is closely associated with breast cancer (BC), with studies by Kim et al. indicating that its knockdown facilitates BC metastasis, suggesting MALAT1 plays an inhibitory role in this process [48]. Data from GEPIA website shows that MALAT1 is lowly expressed in BC. The Chipbase v2.0 website obtained a positive co-expression correlation between MALAT1 and STAT4 in BC (**Figure 4A**), speculating that STAT4 could be a transcription factor for MALAT1. RT-qPCR examination of MALAT1 in clinical samples showed markedly downregulated MALAT1 in BC tissues (**Figure 4B**). In addition, Pearson correlation analysis revealed a positive correlation of MALAT1 with STAT4 expression in BC (**Figure 4C**).

Upon overexpressing STAT4 in MCF-7R cells, a marked increase in MALAT1 expression was observed via RT-qPCR (**Figure 4D**), and ChIP assays showed increased STAT4 binding to the MALAT1 promoter (**Figure 4E**). The DLR assay showed obviously enhanced MALAT1 promoter activity after overexpressing STAT4 (**Figure 4F**). Therefore, STAT4 activates MALAT1 transcription in BC cells through binding to the promoter region of MALAT1.

To further investigate whether STAT4 affects BC cells' resistance to radiotherapy through transcriptional activation of MALAT1, MCF-7R cells were divided into oe-NC+sh-NC, oe-STAT4+sh-NC, and oe-STAT4+sh-MALAT1 groups for study. RT-qPCR demonstrated efficient MALAT1 knockdown, especially with sh-MALAT1#3, which was chosen for subsequent experiments (**Figure 4G**). According to RT-qPCR and WB assays, oe-STAT4+sh-NC group had significantly higher STAT4 and MALAT1 expression than oe-NC+sh-NC group (**Figure 4H**, **4I**). After 4 Gy X-ray irradiation, the cell survival rate (**Figure 4J**), proliferation capacity (**Figure 4K**) were significantly increased in MCF-7R+oe-STAT4+sh-MALAT1 group compared to MCF-7R+oe-STAT4+sh-NC group, while the apoptosis level was reduced (**Figure 4L**).

After subjecting MCF-7R with oe-STAT4+sh-MALAT1 or oe-STAT4+sh-NC to X-ray irradiation of different doses, plate cloning assays were carried out. The results revealed a slower decreased proliferation in MCF-7R oe-STAT4+sh-MALAT1 group with higher irradiation doses (**Figure 4M**).

MALAT1 targets and adsorbs miR-21-5p in BC cells

To unveil the downstream regulating mechanisms of MALAT1 in BC cells' resistance to radiotherapy, we used the StarBase and LncBase databases to predict the downstream miRNAs of MALAT1. We identified 113 and 563 miRNAs from each database, respectively. By intersecting these predictions with BC-related miRNAs, we pinpointed 8 miRNAs, including miR-1297, miR-206, miR-21-5p, and miR-4429 (**Figure 5A**). Notably, miR-21-5p, known to be implicated in the onset and progression of BC [49-51], was selected for further study due to its less-explored role in BC cells' resistance to radiotherapy.

The binding loci of MALAT1 and miR-21-5p were obtained through the StarBase website (**Figure 5B**). RT-qPCR analyses of clinical samples demonstrated high miR-21-5p expression in BC tissues (**Figure 5C**). Pearson correlation analysis

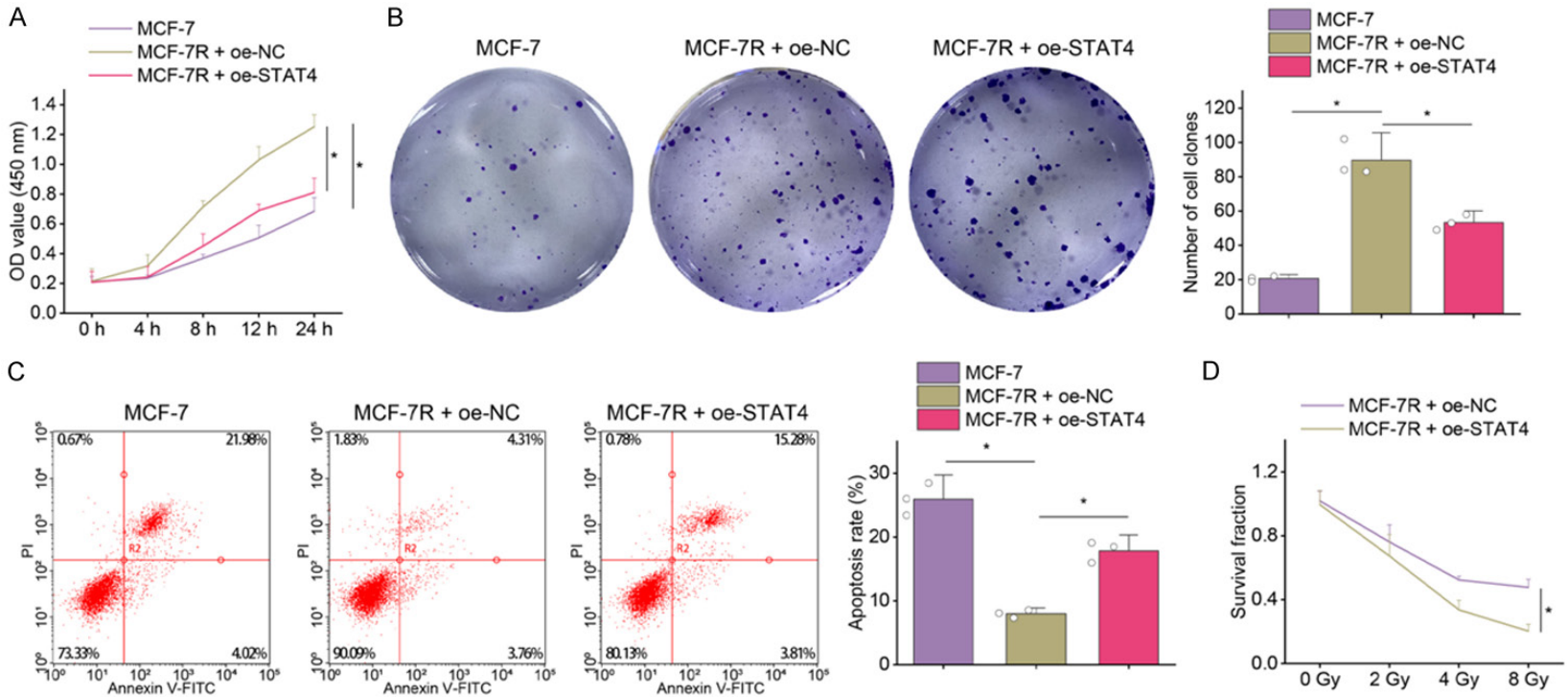

Figure 3. STAT4 overexpression could reverse radiation therapy resistance. A: Cell survival rate by MTT assay, * denotes $P < 0.05$; B: Plate cloning assay to detect cell proliferation ability, * denotes $P < 0.05$; C: Flow cytometry to detect apoptosis, * denotes $P < 0.05$; D: Plate cloning assay to detect changes in MCF-7R proliferating capacity in each group, * denotes $P < 0.05$.

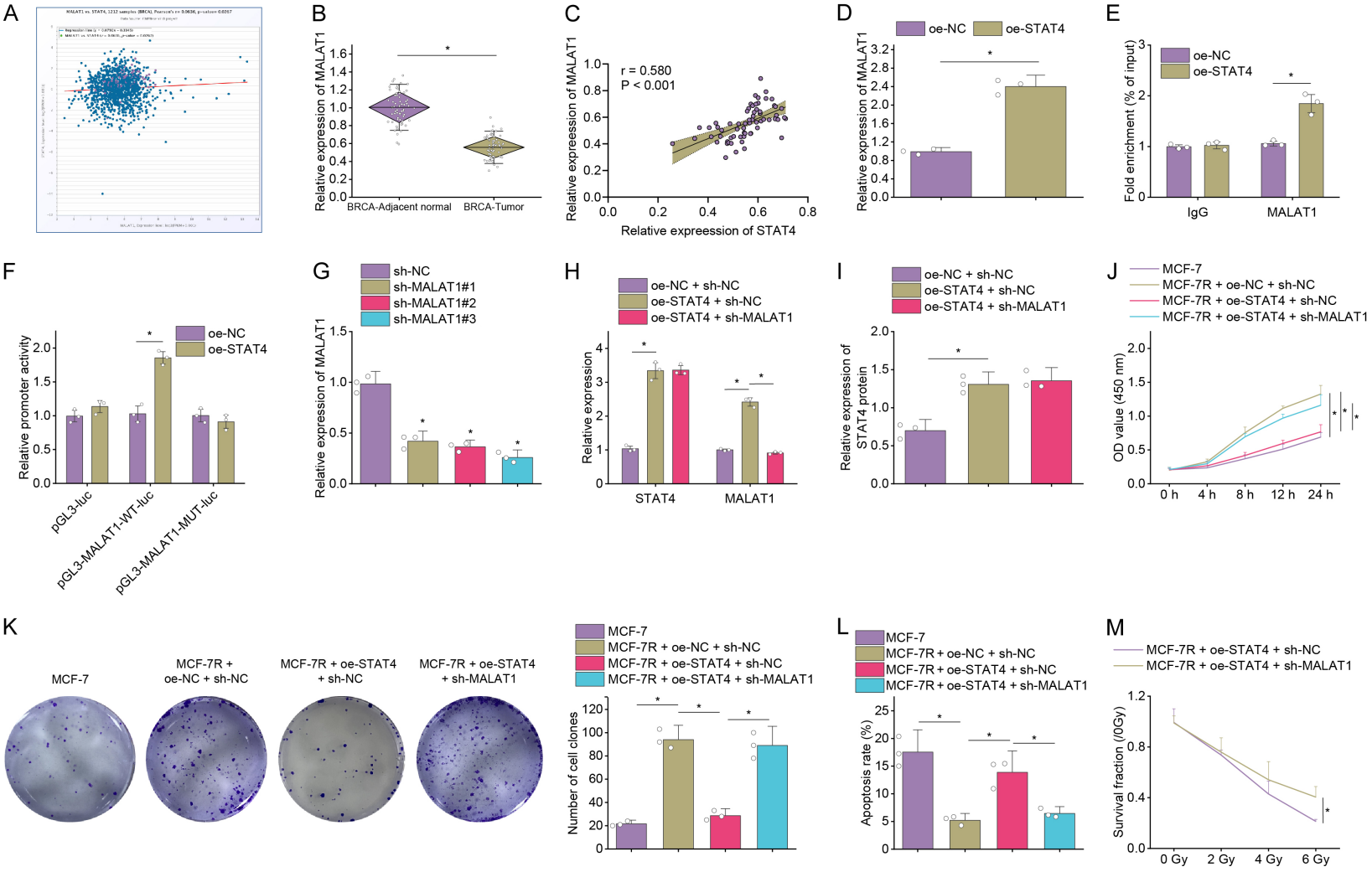

Figure 4. Impact of STAT4 on resistance to radiotherapy through regulation of MALAT1 expression in breast carcinoma (BC) cells. A: Co-expression relationship between STAT4 and MALAT1 in BC; B: RT-qPCR to quantify MALAT1 levels in BC tissues and normal counterparts, n = 66, * indicates comparison with normal tissues adjacent to cancer, *$P < 0.05$; C: Correlation analysis of MALAT1 and STAT4 mRNA levels in 66 BC tissue samples; D: RT-qPCR to quantify MALAT1 in MCF-7R, *$P < 0.05$ versus oe-NC group; E: CHIP assay to detect STAT4-bound MALAT1 in each group of MCF-7R, *$P < 0.05$; F: Dual luciferase reporter assay to measure MALAT1 levels in oe-NC and oe-STAT4-treated 293T cells for MALAT1 promoter activity; G: RT-qPCR assay for knockdown efficiency of three pairs of MALAT1 interference sequences; H: RT-qPCR assay for STAT4 and MALAT1 levels in MCF-7R, *$P < 0.05$; I: Western blot assay for each group of MCF-7R cells, *$P < 0.05$; J: MTT assay to detect MCF-7R cell survival, *$P < 0.05$; K: Plate cloning assay to detect MCF-7R proliferation, *$P < 0.05$; L: Flow cytometry to detect MCF-7R cell apoptosis, *$P < 0.05$; M: Plate cloning assay to identify changes in the proliferative capacity of MCF-7R, *$P < 0.05$.

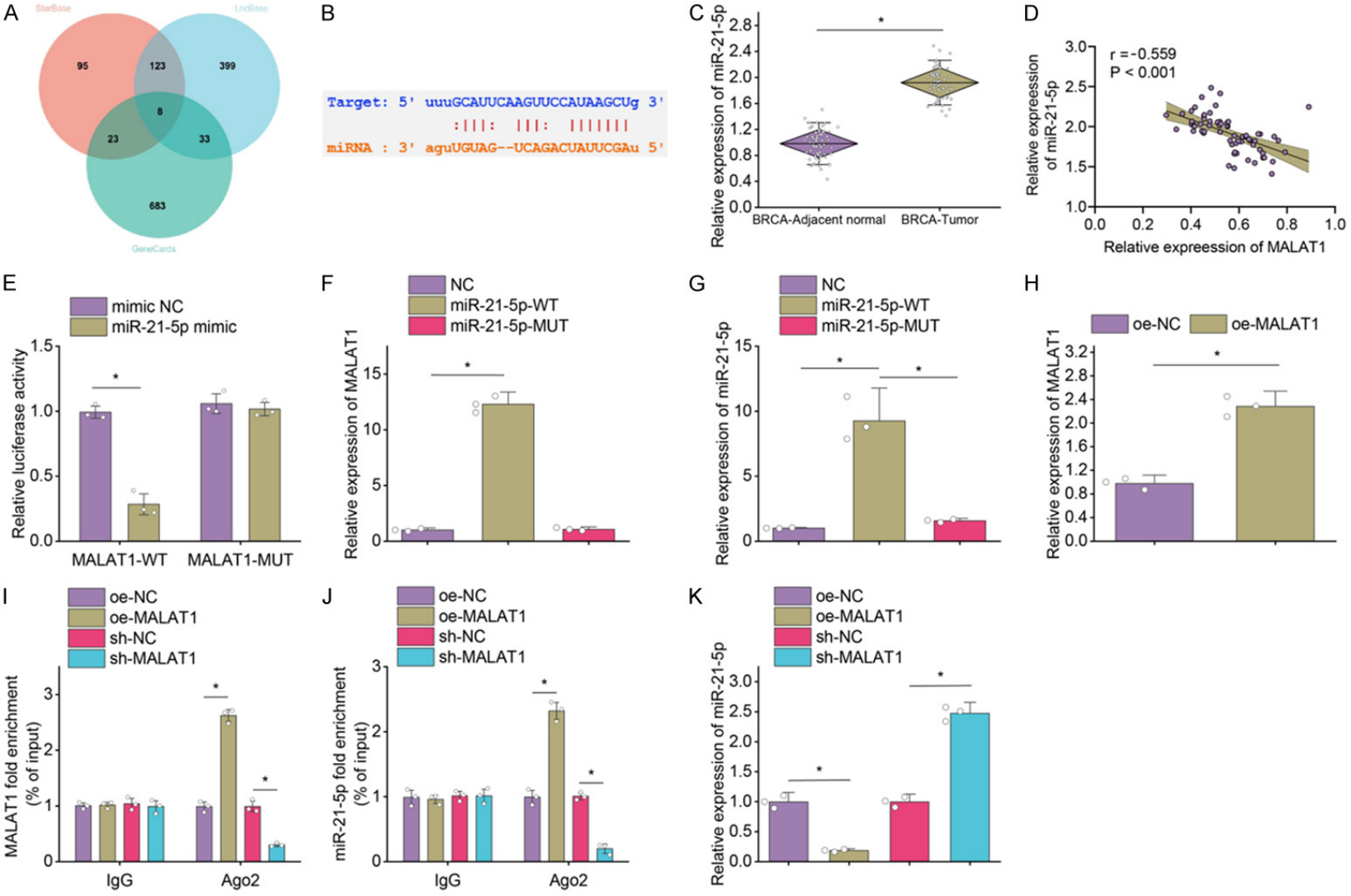

Figure 5. Validation of the targeting correlation between MALAT1 and miR-21-5p in breast carcinoma (BC) cells. A: Venn diagram of StarBase, LncBase predicted miRNAs downstream of MALAT1 and BC-associated miRNAs in GeneCards; B: Diagram of the predicted binding loci of MALAT1 and miR-21-5p by StarBase; C: RT-qPCR detection of miR-21-5p evels in BC tissues and adjacent normal counterparts, n = 66, * indicates comparison with normal counterparts adjacent to cancer, *P < 0.05; D: Correlation analysis of miR-21-5p and MALAT1 in 66 BC tissue samples; E: The targeting correlation between MALAT1 and miR-21-5p by dual luciferase reporter assay, *P < 0.05 versus mimic NC group; F: The binding of biotin-labeled miR-21-5p-WT and mutant sequence miR-21-5p-MUT to MALAT1 by RNA-pull-down assay, *P < 0.05; G: The binding of biotin-labeled MALAT1-WT and mutant sequence MALAT1-MUT to miR-21-5p by RNA-pull-down assay, *P < 0.05; H: RT-qPCR to detect MALAT1 levels in MCF-7R, *P < 0.05 versus oe-NC group; I: RIP assay to detect MALAT1 enrichment within the RISC core element Ago2 in MCF-7R, *P < 0.05; J: RIP assay to detect miR-21-5p enrichment within the RISC core element Ago2 in MCF-7R, *P < 0.05; K: RT-qPCR to quantify miR-21-5p in MCF-7R, *P < 0.05.

revealed an inverse link between miR-21-5p and MALAT1 expression in BC (**Figure 5D**). We cloned both wild-type MALAT1 (with the miR-21-5p binding site) and mutated MALAT1 sequences into a luciferase reporter vector, co-transfecting these with either a miR-21-5p mimic or a negative control mimic. The miR-21-5p mimic significantly reduced luciferase activity compared to the negative control, whereas the mutant MALAT1 did not show a significant difference, highlighting miR-21-5p's specific binding to the MALAT1 sequence (**Figure 5E**). As indicated by the RNA pull-down assay, MALAT1 and miR-21-5p were significantly pulled down by the biotin-labelled miR-21-5p-WT probe and the biotin-labelled MALAT1-WT probe, respectively (**Figure 5F**, **5G**), indicating the ability of MALAT1 to bind to miR-21-5p.

Subsequently, we manipulated the expression of MALAT1 in MCF-7R cells (**Figure 5G**, **5H**). RIP assays indicated a significant increase in the enrichment of both MALAT1 and miR-21-5p within the RNA-induced silencing complex (RISC) core element, Argonaute 2 (Ago2), after MALAT1 overexpression in MCF-7R cells (**Figure 5I**, **5J**). Conversely, disrupting MALAT1 led to a considerable reduction in the enrichment of both MALAT1 and miR-21-5p within Ago2 (**Figure 5I**, **5J**). RT-qPCR results corroborated these findings, showing a notable decrease in miR-21-5p expression subsequent to MALAT1 overexpression and an increase when MALAT1 was interfered with (**Figure 5K**).

MALAT1 up-regulates THRB expression through the adsorption of miR-21-5p

We further predicted miR-21-5p's downstream regulators by intersecting the predicted target genes of miR-21-5p from four websites (miRDB, mirT-CDS, mirDIP and StarBase) and obtained 34 candidate genes, including PPARA, CTSC and THRB (**Figure 6A**). PPARA, THRB, LIFR, NFIB, and RECK are lowly expressed in BC (**Figure 6B**), of which THRB is an oncogene and has been shown to inhibit breast tumour growth [52]. Additionally, miR-21-5p and THRB were found to have a potential binding site via StarBase predictions (**Figure 6C**). Subsequently, we used RT-qPCR and WB to examine THRB levels in clinical samples. Both THRB protein and mRNA levels were notably down-regulated in BC tissues versus paracancerous tissues (**Figure 6D**, **6E**). An inverse correlation was found between THRB and miR-21-5p expression in BC (**Figure 6F**).

THRB-WT (binding site sequence) and THRB-MUT (mutated sequence) of miR-21-5p were cloned into the luciferase reporter vector as a reporter plasmid. Mimic NC and miR-21-5p mimic were co-transfected with THRB luciferase reporter plasmids. The luciferase activity in the THRB-WT plasmid cotransfection group was markedly reduced versus the mimic NC cotransfection group, and the luciferase activity in the miR-21-5p mimic and THRB-MUT plasmid cotransfection group did not alter notably versus the mimic NC cotransfection group (**Figure 6G**). We then interfered miR-21-5p expression in MCF-7R cells (**Figure 6H**) and used RT-qPCR and WB to measure THRB expression in in each group. Upon modulating miR-21-5p expression in MCF-7R cells, overexpression of miR-21-5p was shown to decrease THRB mRNA and protein levels, while miR-21-5p inhibition had the opposite effect (**Figure 6I**, **6J**).

To investigate whether MALAT1 regulates THRB expression through adsorbing miR-21-5p, we overexpressed MALAT1 and miR-21-5p in MCF-7R. The results indicated that MALAT1 overexpression counteracts the effect of miR-21-5p on THRB, leading to increased THRB expression, suggesting a regulatory mechanism of MALAT1 over miR-21-5p in the context of THRB expression (**Figure 6K-N**).

STAT4 regulates THRB expression through the MALAT1/miR-21-5p axis reversing radiation therapy resistance in BC cells

Next, we explored whether STAT4 affects BC cell radiotherapy resistance via modulating the MALAT1/miR-21-5p/THRB axis. We silenced THRB or overexpressed STAT4 in MCF-7R. RT-qPCR and WB assays showed markedly enhanced STAT4, MALAT1 and THRB levels. miR-21-5p was notably underexpressed in oe-STAT4+sh-NC group than in oe-NC+sh-NC group. STAT4, MALAT1 and miR-21-5p levels did not alter markedly in oe-STAT4+sh-THRB group versus oe-STAT4+sh-NC group, while THRB was greatly lowered (**Figure 7A**, **7B**).

MCF-7, as well as MCF-7R from oe-NC+sh-NC, oe-STAT4+sh-NC, and oe-STAT4+sh-THRB

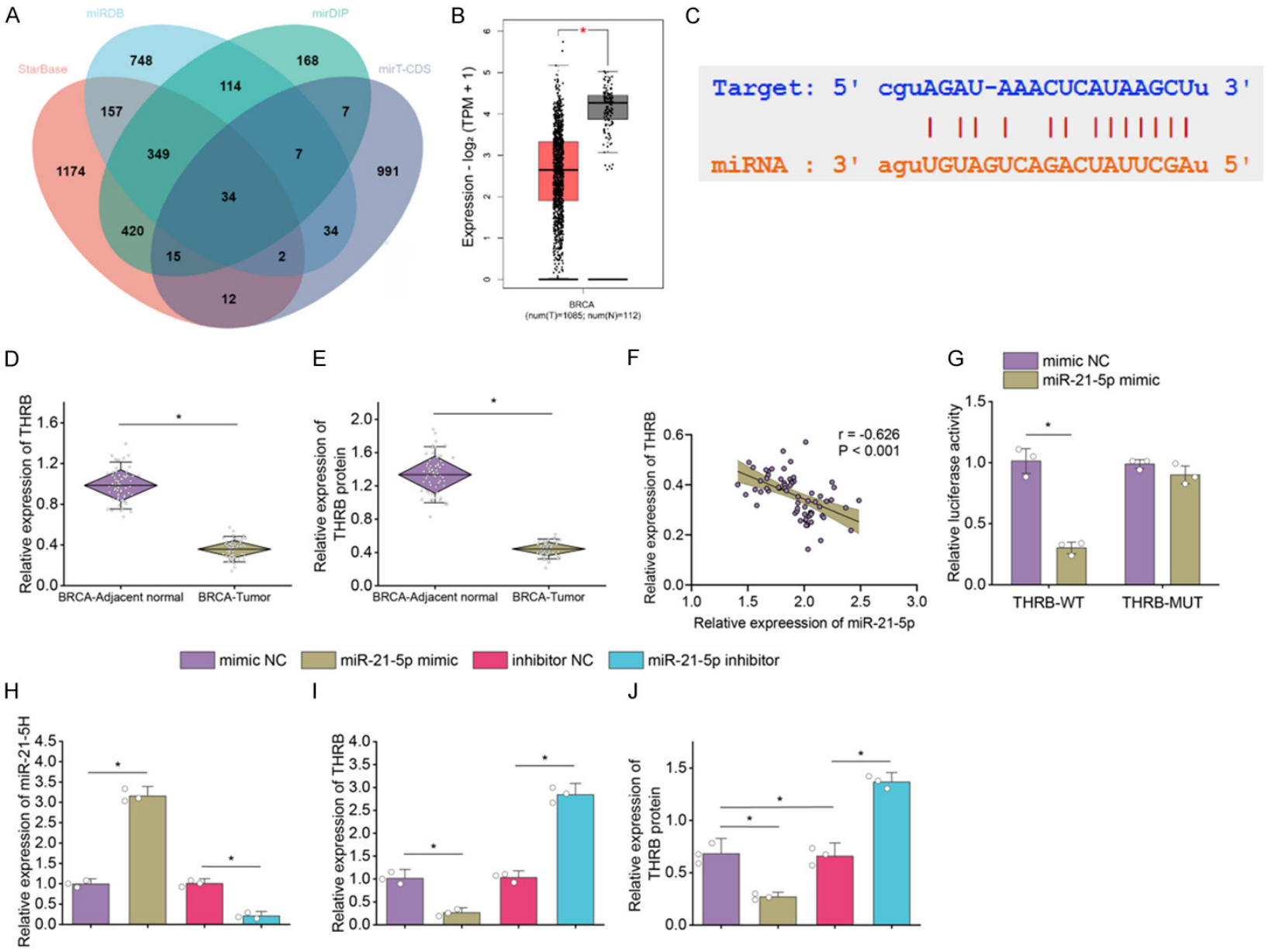
A
miRDB
mirDIP
StarBase
mirT-CDS
748
168
114
157
7
349
7
1174
991
34
420
34
15
2
12
B
Expression - log2 (TPM + 1)
BRCA
(num(T)=1085; num(N)=112)
C
Target: 5' cguAGAU-AAACUCAUAAGCUu 3'
miRNA : 3' aguUGUAGUCAGACUAUUCGAu 5'
D
Relative expression of THRB
BRCA-Adjacent normal
BRCA-Tumor
E
Relative expression of THRB protein
BRCA-Adjacent normal
BRCA-Tumor
F
Relative expression of THRB
r = -0.626
P < 0.001
Relative expression of miR-21-5p
G
mimic NC
miR-21-5p mimic
Relative luciferase activity
THRB-WT
THRB-MUT
mimic NC
miR-21-5p mimic
inhibitor NC
miR-21-5p inhibitor
H
Relative expression of miR-21-5H
I
Relative expression of THRB
J
Relative expression of THRB protein

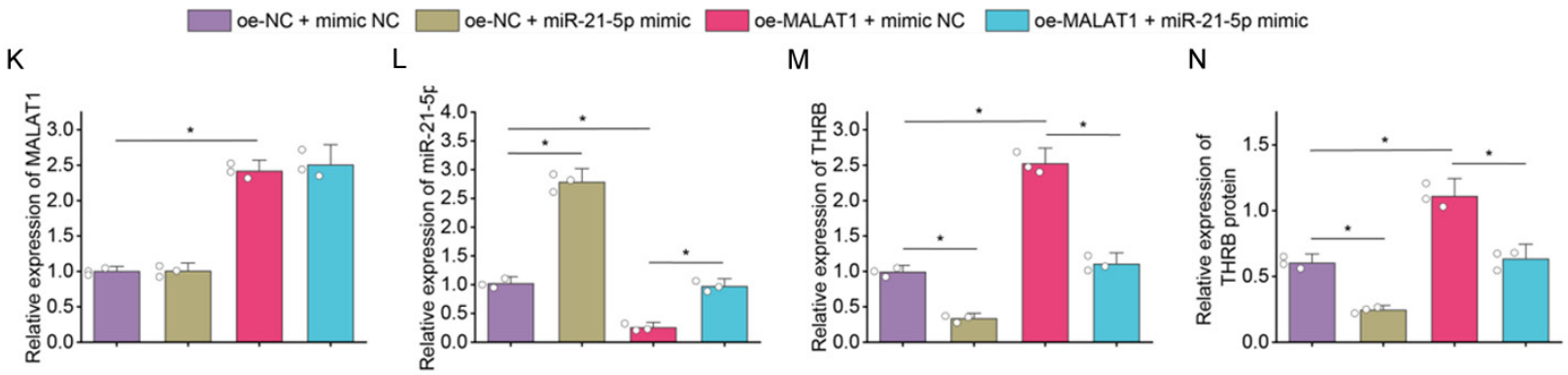

Figure 6. MALAT1 regulates THRB by adsorbing miR-21-5p. A: Venn diagram of the four websites (miRDB, mirT-CDS, mirDIP and StarBase) predicting the miR-21-5p target gene; B: GEPIA website analyzing THRB expression in BC patients; C: StarBase website predicting the target binding loci of miR-21-5p and THRB; D, E: RT-qPCR and Western blot to quantify THRB mRNA and protein levels in cancer tissue and adjacent counterparts, n = 66, *P < 0.05 versus adjacent counterparts; F: Correlation of miR-21-5p and THRB mRNA levels in 66 BC tissue samples; G: Targeting correlation between miR-21-5p and THRB by double luciferase reporter assay, *P < 0.05 versus mimic-NC group; H: RT-qPCR to detect miR-21-5p levels in MCF-7R, *P < 0.05; I, J: RT-qPCR and Western blot to quantify THRB mRNA and protein levels in MCF-7R, *P < 0.05; K, L: RT-qPCR to measure MALAT1 and miR-21-5p levels in MCF-7R, *P < 0.05; M, N: RT-qPCR and Western blot to determine THRB in MCF-7R, *P < 0.05. 7R cells, mRNA and protein expression levels of THRB in each group, *P < 0.05.

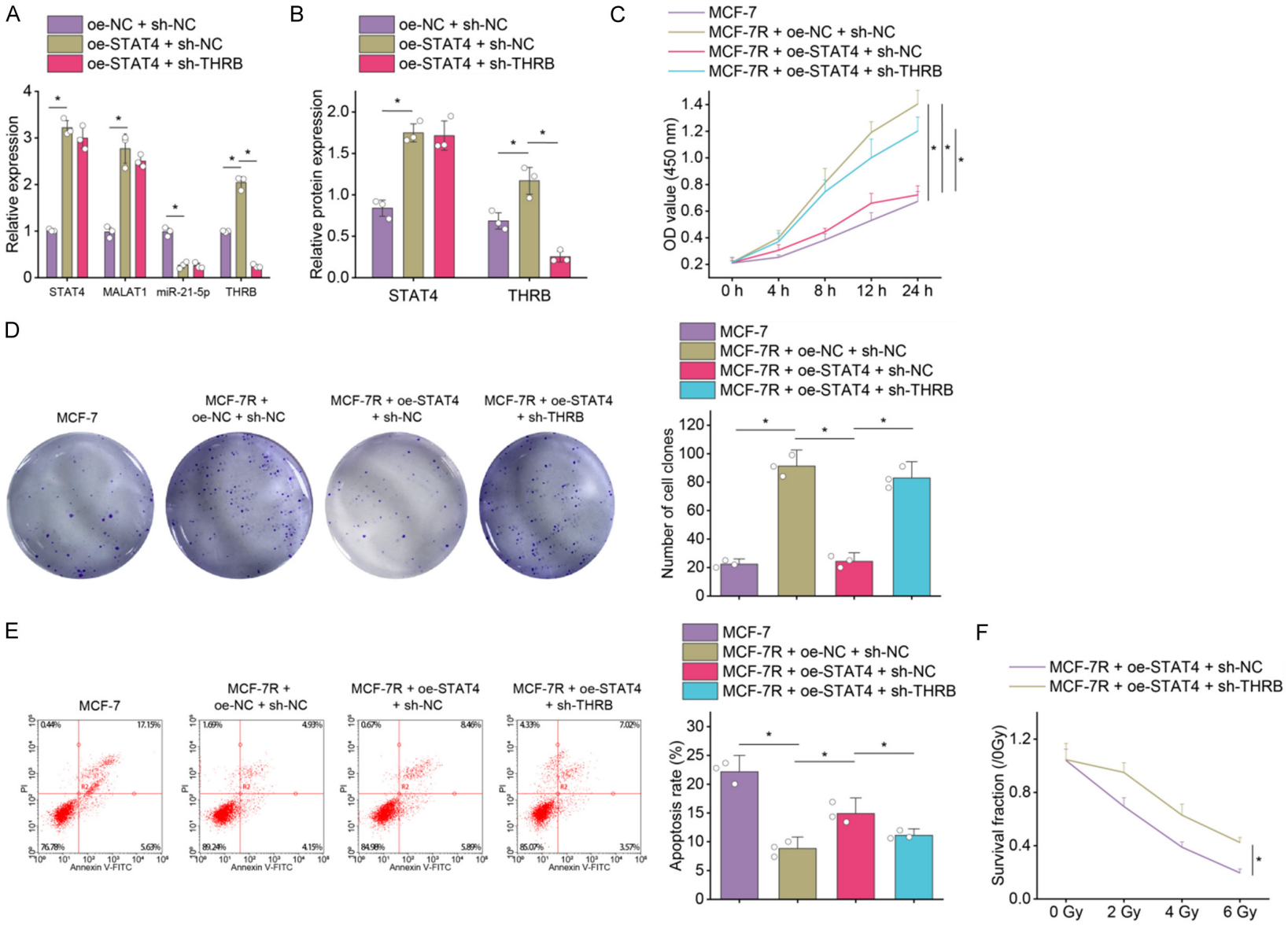

Figure 7. STAT4 regulation of MALAT1/miR-21-5p/THRB axis to influence breast carcinoma (BC) cell resistance to radiotherapy. A: RT-qPCR results indicate STAT4, MALAT1, miR-21-5p and THRB levels in MCF-7R, *$P < 0.05$; B: Western blot reveals STAT4 and THRB protein levels in MCF-7R, *$P < 0.05$; C: MTT assay for cell survival rate, *$P < 0.05$; D: Plate cloning assay on cell proliferating capacity, *$P < 0.05$; E: Flow cytometry about apoptosis level, *$P < 0.05$; F: Plate cloning assay to measure changes in MCF-7R cell proliferating capacity, *$P < 0.05$.

groups were treated with 4 Gy X-ray irradiation. MCF-7R cells from the oe-STAT4+sh-THRB group had a greatly elevated survival rate (**Figure 7C**), a significantly higher proliferation capacity (**Figure 7D**) and a significantly lower level of apoptosis (**Figure 7E**) than MCF-7R from the oe-STAT4+sh-NC group. A plate cloning assay indicated that, with higher irradiation doses, the proliferation of MCF-7R cells in the oe-STAT4+sh-THRB group decreased more slowly (**Figure 7F**).

Overexpression of STAT4 inhibits resistance to radiotherapy in BC by up-regulating THRB expression in animal model

MCF-7 and MCF-7R were grafted to nude mice subcutaneously, and the tumor volume and weight were determined by irradiating the nude mice with 4 Gy X-rays. Notably, the MCF-7R cells with overexpressed STAT4 and silenced negative control (sh-NC) exhibited a substantially reduced tumorigenic capability compared to the standard MCF-7R cells. The tumorigenic ability further declined in the MCF-7R cells with silenced THRB (**Figure 8A-C**).

RT-qPCR, WB and immunohistochemistry showed statistically decreased STAT4, MALAT1 and THRB levels and markedly elevated miR-21-5p in the MCF-7R+oe-NC+sh-NC group compared to the MCF-7 group; STAT4, MALAT1 and THRB were notably elevated and miR-21-5p was noticeably reduced in MCF-7R+oe-NC+sh-NC group compared to MCF-7R+oe-NC+sh-NC group. Obviously increased STAT4, MALAT1 and THRB and statistically reduced miR-21-5p were observed in MCF-7R+oe-STAT4+sh-NC group versus MCF-7R+oe-STAT4+sh-NC group; compared to the MCF-7R+oe-STAT4+sh-NC group, STAT4, miR-21-5p and MALAT1 did not alter significantly while THRB reduced statistically in the MCF-7R+oe/STAT4+sh-THRB group (**Figure 8D-F**).

As indicated by immunohistochemistry and TUNEL staining, the MCF-7R+oe-NC MALAT1 group exhibited notably enhanced cell proliferation and reduced apoptosis than the MCF-7 group; MCF-7R+oe-STAT4+sh-NC group exhibited marked decreases in cell proliferation and apoptosis than MCF-7R+oe-NC MALAT1 group. The MCF-7R+oe-STAT4+sh-NC group showed an evident elevation in cell proliferation and an obvious decline in apoptosis than the MCF-7R+oe-STAT4+sh-THRB group (**Figure 8G**, **8H**).

Therefore, overexpressing STAT4 inhibits miR-21-5p and up-regulates THRB expression through transcriptional activation of MALAT1, thereby suppressing resistance to radiotherapy in BC.

Discussions

Evidence has linked high STAT4 expression to better OS and recurrence-free survival in BC patients [53], as well as elevated STAT4 and IL12B1/2 levels to better survival [54]. In addition, pSTAT4 in $CD4^+$ T cells can be up-regulated by cryptotanshinone, inhibiting BC cell growth in vivo [55]. The genes co-expressed with STAT4 have a substantial presence in adaptive immune responses, highlighting the importance of further exploring the role of STAT4 in BC, particularly within the breast immune microenvironment [56].

Our *in vitro* cellular assays revealed that STAT4 could target MALAT1 through transcriptional activation to adsorb miR-21-5p and up-regulate THRB expression. As shown by *in vitro* cellular assays, the transcription factor STAT4 inhibits BC cell resistance to radiotherapy by binding to the MALAT1 promoter region to upregulate MALAT1 levels. Further analysis showed that MALAT1 up-regulates THRB expression by adsorbing miR-21-5p. The activation of MALAT1 has also been found to suppress BC metastasis and, conversely, its inactivation promotes metastasis [57]. In addition, MALAT1 could target miR-485-3p to modulate BC cell resistance to paclitaxel chemotherapy, thus achieving MALAT1 inhibition in BC cells [58].

Our study indicates that STAT4's overexpression counteracts BC cell resistance to radiotherapy through the MALAT1/miR-21-5p/THRB axis, with in vitro experiments supporting STAT4's role as a positive regulator of MALAT1. In vitro experiments suggest the role of STAT4 as a positive regulator of MALAT1, and overexpressing MALAT1 inhibits miR-21-5p, a negative regulator of THRB. Thus STAT4 inhibits BC cell resistance to radiotherapy via modulating MALAT1/miR-21-5p/THRB, which was consistent with previous study [1]. High MALAT1 expression inhibited BC progression suppressing its metastasis [59]. Furthermore, miR-21-5p, positively linked to BC development, is a biomarker for BC diagnosis [60]. Suppressing miR-21-5p inhibited BC progression [61]. In addition, high THRB expression weakened the

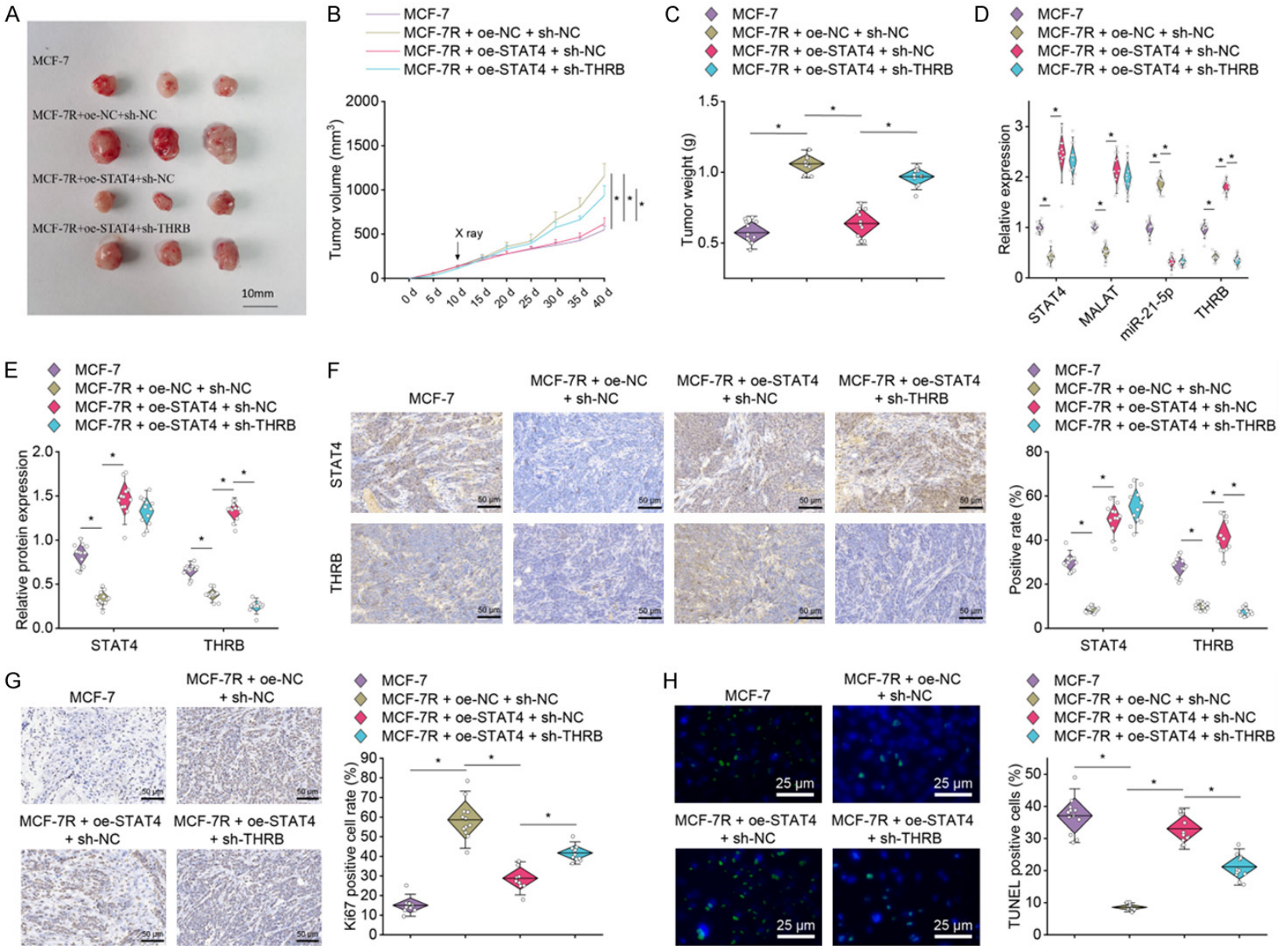
A
MCF-7
MCF-7R+oe-NC+sh-NC
MCF-7R+oe-STAT4+sh-NC
MCF-7R+oe-STAT4+sh-THRB
10mm
B
MCF-7
MCF-7R + oe-NC + sh-NC
MCF-7R + oe-STAT4 + sh-NC
MCF-7R + oe-STAT4 + sh-THRB
Tumor volume (mm3)
X ray
0 d
5 d
10 d
15 d
20 d
25 d
30 d
35 d
40 d
C
Tumor weight (g)
D
Relative expression
STAT4
MALAT
miR-21-5p
THRB
E
Relative protein expression
STAT4
THRB
F
MCF-7
MCF-7R + oe-NC + sh-NC
MCF-7R + oe-STAT4 + sh-NC
MCF-7R + oe-STAT4 + sh-THRB
STAT4
THRB
50 μm
Positive rate (%)
G
Ki67 positive cell rate (%)
H
25 μm
TUNEL positive cells (%)

Figure 8. The in vivo validation of the STAT4-regulated MALAT1/miR-21-5p/THRB axis and its effect on breast carcinoma cell radiotherapy resistance. A: Representative images of tumors in each group, bar = 10 mm; B: Tumor change curves, *$P < 0.05$; C: Comparison of tumor weight, *$P < 0.05$; D: RT-qPCR for measuring STAT4, THRB, miR-21-5p and MALAT1 levels in solid tumors, *$P < 0.05$; E: Western blot reveals STAT4 and THRB protein levels in solid tumors, *$P < 0.05$; F: Immunohistochemistry shows STAT4 and THRB protein levels in solid tumors, *$P < 0.05$; G: Immunohistochemistry on ki67 levels in solid tumors, *$P < 0.05$; H: TUNEL staining to determine apoptosis, *$P < 0.05$; n = 12.

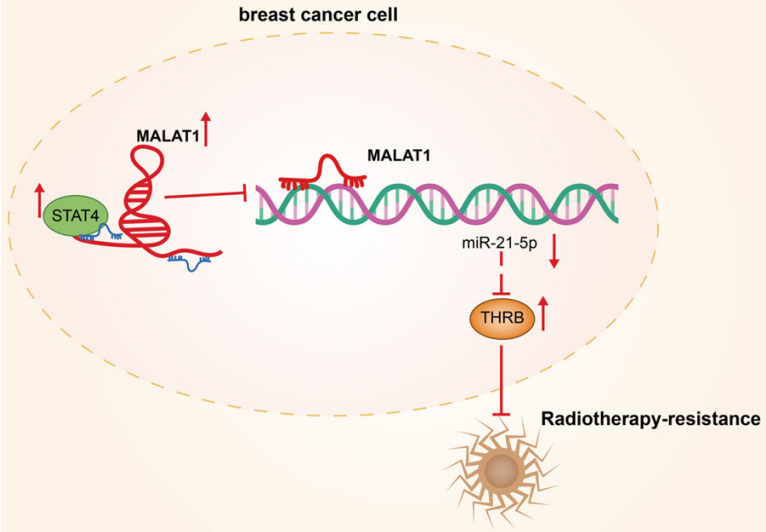

Figure 9. The molecular mechanism by which STAT4 counteracts miR-21-5p and enhances THRB expression via the transcriptional activation of MALAT1, effectively reversing radiotherapy resistance in breast carcinoma cells.

proliferative potential of cells in vitro and promoted cell death in concert with radiotherapy, improving the efficacy of radiotherapy [62].

In vivo animal studies corroborate the capability of STAT4 overexpression to reverse BC cell resistance to radiotherapy and suppress tumor formation by upregulating THRB expression. There is growing evidence that signal transducer and activator of transcription (STAT) proteins, known as cytoplasmic transcription factors, play a key part in multiple cell biological processes and may be prognostic predictors for certain cancers. THRB is proposed to act as an anti-oncogene for BC development [63]. The relationship between overexpression of STAT4 and BC has been reported, where STAT4 expression was activated with an increase in the cytotoxic $CD4^+$ T cell count, promoting their anti-BC function [55]. In addition, high expression of THRB cooperated with radiotherapy to reduce the proliferative potential of tumour cells and promote cell death, enhancing the efficacy of radiotherapy [62].

In conclusion, our research tentatively posits STAT4 is a positive regulator directly targeted by MALAT1, which in turn is negatively regulated by miR-21-5p, with low miR-22-3p expression influencing THRB up-regulation. The transcription factor STAT4 inhibits miR-21-5p and up-regulates THRB expression through transcriptional activation of MALAT1, thereby reversing BC cell radiotherapy resistance and preventing BC occurrence and progression (**Figure 9**). Still, there are several limitations: MALAT1 interacts with a variety of miRNAs, warranting further exploration of its downstream targets. Moreover, the clinical application of STAT4 agonists alongside radiotherapy treatment requires additional investigation into feasibility and safety.

Acknowledgements

A Study on the Open Teaching Method Combined with Scientific Research - Taking the Course of Radiotherapy Target Area Mapping as an Example (Wjlx2021332); Immune Radiotherapy Research Fund Project of the Radiation Tumor Treatment Credit Committee of the Chinese Medical Association (Z-2017-24-2108).

Disclosure of conflict of interest

None.

Address correspondence to: Leiming Guo, Department of Radiation, The Affiliated Cancer Hospital of Zhengzhou University & Henan Cancer Hospital, No. 127 Dongming Road, Zhengzhou 450008, Henan, China. Tel: +86-400-0371-818; E-mail: guoguo19-801128@163.com

References

[1] Aghiorghiesei O, Zanoaga O, Raduly L, Aghiorghiesei AI, Chiroi P, Trif A, Buiga R, Budisan L, Lucaciu O, Pop LA, Braicu C, Campian R and Berindan-Neagoe I. Dysregulation of miR-21-5p, miR-93-5p, miR-200c-3p and miR-205-5p in oral squamous cell carcinoma: a potential biomarkers panel? Curr Issues Mol Biol 2022; 44: 1754-1767.

[2] Siegel RL, Miller KD, Fuchs HE and Jemal A. Cancer statistics, 2021. CA Cancer J Clin 2021; 71: 7-33.

[3] Barzaman K, Karami J, Zarei Z, Hosseinzadeh A, Kazemi MH, Moradi-Kalbolandi S, Safari E and Farahmand L. Breast cancer: biology, biomarkers, and treatments. Int Immunopharmacol 2020; 84: 106535.

[4] Al-Hajj M, Wicha MS, Benito-Hernandez A, Morrison SJ and Clarke MF. Prospective identification of tumorigenic breast cancer cells. Proc Natl Acad Sci U S A 2003; 100: 3983-3988.

[5] Aggarwal S, Verma SS, Aggarwal S and Gupta SC. Drug repurposing for breast cancer therapy: old weapon for new battle. Semin Cancer Biol 2021; 68: 8-20.

[6] Yang C, Mai H, Peng J, Zhou B, Hou J and Jiang D. STAT4: an immunoregulator contributing to diverse human diseases. Int J Biol Sci 2020; 16: 1575-1585.

[7] Kaplan MH. STAT4: a critical regulator of inflammation in vivo. Immunol Res 2005; 31: 231-242.

[8] Walker JG, Ahern MJ, Coleman M, Weedon H, Papangelis V, Beroukas D, Roberts-Thomson PJ and Smith MD. Characterisation of a dendritic cell subset in synovial tissue which strongly expresses Jak/STAT transcription factors from patients with rheumatoid arthritis. Ann Rheum Dis 2007; 66: 992-999.

[9] Wang S, Yu L, Shi W, Li X and Yu L. Prognostic roles of signal transducers and activators of transcription family in human breast cancer. Biosci Rep 2018; 38: BSR20171175.

[10] Zhou Y, Jiang S, Yu S, Zhu L, Liu Y, Li S, Hao N and Ren Y. Mining the prognostic significance and immune infiltration of STAT family members in human breast cancer by bioinformatics analysis. Gland Surg 2022; 11: 720-741.

[11] Zhu H, Wang Z, Xu Q, Zhang Y, Zhai Y, Bai J, Liu M, Hui Z and Xu N. Inhibition of STAT1 sensitizes renal cell carcinoma cells to radiotherapy and chemotherapy. Cancer Biol Ther 2012; 13: 401-407.

[12] Hui Z, Tretiakova M, Zhang Z, Li Y, Wang X, Zhu JX, Gao Y, Mai W, Furge K, Qian CN, Amato R, Butler EB, Teh BT and Teh BS. Radiosensitization by inhibiting STAT1 in renal cell carcinoma. Int J Radiat Oncol Biol Phys 2009; 73: 288-295.

[13] Bonner JA, Trummell HQ, Willey CD, Plants BA and Raisch KP. Inhibition of STAT-3 results in radiosensitization of human squamous cell carcinoma. Radiother Oncol 2009; 92: 339-344.

[14] Li ZX, Zhu QN, Zhang HB, Hu Y, Wang G and Zhu YS. MALAT1: a potential biomarker in cancer. Cancer Manag Res 2018; 10: 6757-6768.

[15] Goyal B, Yadav SRM, Awasthee N, Gupta S, Kunnumakkara AB and Gupta SC. Diagnostic, prognostic, and therapeutic significance of long non-coding RNA MALAT1 in cancer. Biochim Biophys Acta Rev Cancer 2021; 1875: 188502.

[16] Sun Q, Hao Q and Prasanth KV. Nuclear long noncoding RNAs: key regulators of gene expression. Trends Genet 2018; 34: 142-157.

[17] Kim J, Piao HL, Kim BJ, Yao F, Han Z, Wang Y, Xiao Z, Siverly AN, Lawhon SE, Ton BN, Lee H, Zhou Z, Gan B, Nakagawa S, Ellis MJ, Liang H, Hung MC, You MJ, Sun Y and Ma L. Long noncoding RNA MALAT1 suppresses breast cancer metastasis. Nat Genet 2018; 50: 1705-1715.

[18] Wang G, Duan P, Liu F and Wei Z. Long noncoding RNA CASC7 suppresses malignant behaviors of breast cancer by regulating miR-21-5p/FASLG axis. Bioengineered 2021; 12: 11555-11566.

[19] Li N, Wang X, Sun J, Liu Y, Han A, Lin Z and Yang Y. miR-21-5p/Tiam1-mediated glycolysis reprogramming drives breast cancer progression via enhancing PFKL stabilization. Carcinogenesis 2022; 43: 705-715.

[20] Chen C, Liu X, Chen C, Chen Q, Dong Y and Hou B. Clinical significance of let-7a-5p and miR-21-5p in patients with breast cancer. Ann Clin Lab Sci 2019; 49: 302-308.

[21] Liu M, Mo F, Song X, He Y, Yuan Y, Yan J, Yang Y, Huang J and Zhang S. Exosomal hsa-miR-21-5p is a biomarker for breast cancer diagnosis. PeerJ 2021; 9: e12147.

[22] Tao L, Wu YQ and Zhang SP. MiR-21-5p enhances the progression and paclitaxel resistance in drug-resistant breast cancer cell lines by targeting PDCD4. Neoplasma 2019; 66: 746-755.

[23] Bernal J. Thyroid hormones in brain development and function. In: Feingold KR, Anawalt B, Blackman MR, Boyce A, Chrousos G, Corpas E, de Herder WW, Dhatariya K, Dungan K, Hofland J, Kalra S, Kaltsas G, Kapoor N, Koch C, Kopp P, Korbonits M, Kovacs CS, Kuohung W, Laferrère B, Levy M, McGee EA, McLachlan R, New M, Purnell J, Sahay R, Shah AS, Singer F, Sperling MA, Stratakis CA, Trence DL, Wilson DP, editors. Endotext. South Dartmouth (MA): MDText.com, Inc. Copyright © 2000-2024, MDText.com, Inc.; 2000.

[24] Ma H, de Zwaan E, Guo YE, Cejas P, Thiru P, van de Bunt M, Jeppesen JF, Syamala S,

Dall'Agnese A, Abraham BJ, Fu D, Garrett-Engele C, Lee TI, Long HW, Griffith LG, Young RA and Jaenisch R. The nuclear receptor THRB facilitates differentiation of human PSCs into more mature hepatocytes. Cell Stem Cell 2022; 29: 795-809, e11.

[25] Kim WG and Cheng SY. Thyroid hormone receptors and cancer. Biochim Biophys Acta 2013; 1830: 3928-3936.

[26] Ling Y, Li Q, Yang H, Wang Y, Tang F, Kang H and Wang Y. Loss of heterozygosity in thyroid hormone receptor beta in invasive breast cancer. Tumori 2015; 101: 572-577.

[27] Wang C, Wang Q and Weng Z. LINC00664/miR-411-5p/KLF9 feedback loop contributes to the human oral squamous cell carcinoma progression. Oral Dis 2023; 29: 672-685.

[28] Wang B, Chen H, Yang R, Xing L, Chen C and Chen J. LncRNA RP11-551L14.4 suppresses breast cancer development by inhibiting the expression of miR-4472. PeerJ 2022; 10: e14482.

[29] Wang J, Polaki V, Chen S and Bihl JC. Exercise improves endothelial function associated with alleviated inflammation and oxidative stress of perivascular adipose tissue in type 2 diabetic mice. Oxid Med Cell Longev 2020; 2020: 8830537.

[30] Salem M, Shan Y, Bernaudo S and Peng C. miR-590-3p targets cyclin G2 and FOXO3 to promote ovarian cancer cell proliferation, invasion, and spheroid formation. Int J Mol Sci 2019; 20: 1810.

[31] Luo W, Liu W, Yao J, Zhu W, Zhang H, Sheng Q, Wang L, Lv L and Qian L. Downregulation of H19 decreases the radioresistance in esophageal squamous cell carcinoma cells. Onco Targets Ther 2019; 12: 4779-4788.

[32] Tian W, Du Y, Ma Y, Gu L, Zhou J and Deng D. MALAT1-miR663a negative feedback loop in colon cancer cell functions through direct miRNA-lncRNA binding. Cell Death Dis 2018; 9: 857.

[33] Luo LL, Zhao L, Wang YX, Tian XP, Xi M, Shen JX, He LR, Li QQ, Liu SL, Zhang P, Xie D and Liu MZ. Insulin-like growth factor binding protein-3 is a new predictor of radiosensitivity on esophageal squamous cell carcinoma. Sci Rep 2015; 5: 17336.

[34] Wang Q, Fan W, Liang B, Hou B, Jiang Z and Li C. YY1 transcription factor induces proliferation and aerobic glycolysis of neuroblastoma cells via LDHA regulation. Exp Ther Med 2022; 25: 37.

[35] Zhang Z, Wu W, Jiao H, Chen Y, Ji X, Cao J, Yin F and Yin W. Squalene epoxidase promotes hepatocellular carcinoma development by activating STRAP transcription and TGF-β/SMAD signalling. Br J Pharmacol 2023; 180: 1562-1581.

[36] Bierhoff H. Analysis of lncRNA-protein interactions by RNA-protein pull-down assays and rna immunoprecipitation (RIP). Methods Mol Biol 2018; 1686: 241-250.

[37] Yu W, Ma L and Li X. DANCR promotes glioma cell autophagy and proliferation via the miR-33b/DLX6/ATG7 axis. Oncol Rep 2023; 49: 39.

[38] Yang Z, Li J, Feng G, Gao S, Wang Y, Zhang S, Liu Y, Ye L, Li Y and Zhang X. MicroRNA-145 modulates N(6)-methyladenosine levels by targeting the 3'-untranslated mRNA region of the N(6)-methyladenosine binding YTH domain family 2 protein. J Biol Chem 2017; 292: 3614-3623.

[39] Huang M, Wang H, Hu X and Cao X. lncRNA MALAT1 binds chromatin remodeling subunit BRG1 to epigenetically promote inflammation-related hepatocellular carcinoma progression. Oncoimmunology 2019; 8: e1518628.

[40] Chang J, Xu W, Du X and Hou J. MALAT1 silencing suppresses prostate cancer progression by upregulating miR-1 and downregulating KRAS. Onco Targets Ther 2018; 11: 3461-3473.

[41] Liccia M and Tournut B. Role of the circulating nurse and the instrument nurse in proctologic surgery. Soins Chir 1986; 36-38.

[42] Pan F, Mao H, Bu F, Tong X, Li J, Zhang S, Liu X, Wang L, Wu L, Chen R, Wei H, Li B, Li C, Yang Y, Steer CJ, Zhao J and Guo Y. Sp1-mediated transcriptional activation of miR-205 promotes radioresistance in esophageal squamous cell carcinoma. Oncotarget 2017; 8: 5735-5752.

[43] Chen Y, Liu Y, Jiang K, Wen Z, Cao X and Wu S. Linear ubiquitination of LKB1 activates AMPK pathway to inhibit NLRP3 inflammasome response and reduce chondrocyte pyroptosis in osteoarthritis. J Orthop Translat 2022; 39: 1-11.

[44] Mirzayans R and Murray D. Do TUNEL and other apoptosis assays detect cell death in preclinical studies? Int J Mol Sci 2020; 21: 9090.

[45] Gong X and Liu X. In-depth analysis of the expression and functions of signal transducers and activators of transcription in human ovarian cancer. Front Oncol 2022; 12: 1054647.

[46] Dong Z, Chen Y, Yang C, Zhang M, Chen A, Yang J and Huang Y. STAT gene family mRNA expression and prognostic value in hepatocellular carcinoma. Onco Targets Ther 2019; 12: 7175-7191.

[47] Li J, Liang L, Liu Y, Luo Y, Liang X, Luo D, Feng Z, Dang Y, Yang L and Chen G. Clinicopathological significance of STAT4 in hepatocellular carcinoma and its effect on cell growth and apoptosis. Onco Targets Ther 2016; 9: 1721-1734.

[48] Yue X, Wu WY, Dong M and Guo M. LncRNA MALAT1 promotes breast cancer progression and doxorubicin resistance via regulating miR-570-3p. Biomed J 2021; 44 Suppl 2: S296-S304.
[49] Baldasici O, Balacescu L, Cruceriu D, Roman A, Lisencu C, Fetica B, Visan S, Cismaru A, Jurj A, Barbu-Tudoran L, Pileczki V, Vlase L, Tudoran O and Balacescu O. Circulating small EVs miRNAs as predictors of pathological response to neo-adjuvant therapy in breast cancer patients. Int J Mol Sci 2022; 23: 12625.
[50] Babadag S, Altundag-Erdogan Ö, Akkaya-Ulum YZ and Çelebi-Saltik B. The role of telocytes and miR-21-5p in tumorigenicity and metastasis of breast cancer stem cells. Mol Biol Rep 2024; 51: 395.
[51] Li J, Huang L, He Z, Chen M, Ding Y, Yao Y, Duan Y, Zixuan L, Qi C, Zheng L, Li J, Zhang R, Li X, Dai J, Wang L and Zhang QQ. Andrographolide suppresses the growth and metastasis of luminal-like breast cancer by inhibiting the NF-κB/miR-21-5p/PDCD4 signaling pathway. Front Cell Dev Biol 2021; 9: 643525.
[52] Park JW, Zhao L and Cheng SY. Inhibition of estrogen-dependent tumorigenesis by the thyroid hormone receptor β in xenograft models. Am J Cancer Res 2013; 3: 302-311.
[53] Zhou J, Wan F, Wang L, Peng C, Huang R and Peng F. STAT4 facilitates PD-L1 level via IL-12R/JAK2/STAT3 axis and predicts immunotherapy response in breast cancer. MedComm (2020) 2023; 4: e464.
[54] Núñez-Marrero A. Assessing the role of the interleukin-12/STAT4 axis in breast cancer by a bioinformatics approach. Int J Sci Basic Appl Res 2019; 48: 38-52.
[55] Zhou J, Xu XZ, Hu YR, Hu AR, Zhu CL and Gao GS. Cryptotanshinone induces inhibition of breast tumor growth by cytotoxic CD4+ T cells through the JAK2/STAT4/ perforin pathway. Asian Pac J Cancer Prev 2014; 15: 2439-2445.
[56] Mirlekar B. Co-expression of master transcription factors determines CD4(+) T cell plasticity and functions in auto-inflammatory diseases. Immunol Lett 2020; 222: 58-66.
[57] Sun Z, Liu J and Liu J. The expression of lncRNA-MALAT1 in breast cancer patients and its influences on prognosis. Cell Mol Biol (Noisy-le-grand) 2020; 66: 72-78.
[58] Aini S, Yan H, Ding W, Adi L and Su P. Long-chain non-coding RNA MALAT1 regulates paclitaxel resistance of breast cancer cells by targeting miR-485-3p. Nan Fang Yi Ke Da Xue Xue Bao 2020; 40: 698-702.
[59] Sun Y and Ma L. New insights into long noncoding RNA MALAT1 in cancer and metastasis. Cancers (Basel) 2019; 11: 216.
[60] Luo T, Liu Q, Tan A, Duan L, Jia Y, Nong L, Tang J, Zhou W, Xie W, Lu Y, Yu Q and Liu Y. Mesenchymal stem cell-secreted exosome promotes chemoresistance in breast cancer via enhancing miR-21-5p-mediated S100A6 expression. Mol Ther Oncolytics 2020; 19: 283-293.
[61] Zhang Y, Wang Y, Xue J, Liang W, Zhang Z, Yang X, Qiao Z, Jiang Y, Wang J, Cao X and Chen P. Co-treatment with miR-21-5p inhibitor and Aurora kinase inhibitor reversine suppresses breast cancer progression by targeting sprouty RTK signaling antagonist 2. Bioengineered 2022; 13: 455-468.
[62] Matsuse M, Saenko V, Sedliarou I, Rogounovitch T, Nakazawa Y, Mitsutake N, Akulevich N, Namba H and Yamashita S. A novel role for thyroid hormone receptor beta in cellular radiosensitivity. J Radiat Res 2008; 49: 17-27.
[63] Zheng Y, Shao X, Huang Y, Shi L, Chen B, Wang X, Yang H, Chen Z and Zhang X. Role of estrogen receptor in breast cancer cell gene expression. Mol Med Rep 2016; 13: 4046-4050.